matrix element sum

$$A'=\frac{2}{m_0}\sum_{j}^{\Gamma_{15}}{}'\frac{|\langle s|p_x|u_j\rangle|^2}{(E_c-E_j)},\tag{C1}$$

where the summation is over all states u_j transforming like Γ_{15}. The prime on the summation means that states in the four-dimensional subspace are not summed over. E_c is the energy of the Γ_1 state at the bottom of the conduction band. The x component of the momentum operator is represented by p_x, and s represents a function transforming like an atomic s function under the tetrahedral group. By using values of M and L' determined for InSb, we can estimate the values of $b_4{}^2M$ and $c_4{}^2L'$. The quantity M appearing in Eq. (13) is defined as

$$M\equiv H_1+H_2,\tag{C2}$$

where H_1 is defined in Eq. (45) and

$$H_2=\frac{2}{m_0}\sum_{j}^{\Gamma_{25}}\frac{|\langle x|p_y|u_j\rangle|^2}{(E_v-E_j)}.\tag{C3}$$

The Γ_{25} levels are expected to be far removed from Γ_{15}, and thus we consider $H_2\approx 0$. The value of H_1 is not known for GaSb. In InSb, H_1 is of the order -5.[31] For the purpose of evaluating terms in u, we assume $H_1\approx -5$, and therefore, $M\approx -5$. The quantity L' is defined as

$$L'\equiv F'+2G,\tag{C4}$$

where

$$F'=\frac{2}{m_0}\sum_{j}^{\Gamma_1}{}'\frac{|\langle x|p_x|u_j\rangle|^2}{(E_v-E_j)}\tag{C5}$$

and G was defined in Eq. (46). We assume that F' makes a negligible contribution to L'. In InSb, $G\approx -1$,[31] and we adopt this value to estimate the size of L'. Thus, using Eq. (13), a value of $u=-2.1$ gives $A'\approx -3.2$; and $u=+1$ gives $A'\approx 0$. The magnitude of A' has not been previously determined experimentally in any semiconductors. Kane[22] has suggested that A' is small compared to P^2/E_g. In the work of Groves *et al.*,[41] the value of A' in HgTe has been taken as zero. Our estimates of A' based on SdH frequency data thus appear to be reasonable.

---

[41] S. H. Groves, R. N. Brown, and C. R. Pidgeon, Phys. Rev. **161**, 779 (1967).

PHYSICAL REVIEW VOLUME 183, NUMBER 3 15 JULY 1969

Donor-Acceptor Pair Lines in Cadmium Sulfide

C. H. Henry, R. A. Faulkner, and K. Nassau
Bell Telephone Laboratories, Murray Hill, New Jersey 07974

(Received 10 March 1969)

We report the first observation of donor-acceptor pair lines in CdS. The spectrum correlates with a distant pair peak at 5176 Å, an I_1 line at 4888.52 Å, and an I_2 line at 4869.30 Å. Several other pair-line spectra were observed in the vapor-grown undoped platelets used in these experiments. One of these correlated with the same I_1 line and distant pair peak, but with an I_2 line at 4869.17 Å. Zeeman experiments confirmed that these lines were donor-acceptor pair lines. The Zeeman pattern of the pair lines could be predicted, using a crystal field and a j-j coupling constant. These constants were determined by the splittings of the pair lines in zero field. For $\mathbf{H}\|c$, the hole g value was the same as for an isolated acceptor. A theoretical wurtzite spectrum was calculated on the basis of Coulomb interactions. The spectrum was much more complicated than a theoretical zinc-blende spectrum and was sensitive to both the dielectric-constant ratio $\epsilon_\perp/\epsilon_\parallel$ and the c/a ratio of the CdS lattice. The experimental lines could not be assigned, but the line densities were in agreement with what was expected for a pair-line spectrum involving a simple donor and acceptor.

I. INTRODUCTION

The edge emission in a semiconductor refers to the emission bands which occur with energies within a few tenths of an eV below the band gap.[1] Of all the II-VI semiconductors, the edge emission has been most extensively studied in CdS, where the emission is in the blue and the green. The "blue edge" consists of sharp line emission from free and bound excitons and phonon replicas of these emission lines. Many of the prominent blue-edge emission lines have been classified by Thomas and Hopfield.[2] The most prominent of these are I_1 lines, which correspond to excitons bound to neutral acceptors, and I_2 lines, which correspond to excitons bound to neutral donors.

The "green-edge" emission in CdS consists of bands about 12-meV wide followed by a series of longitudinal

---

[1] Work on the edge emission in II-VI compounds has been reviewed by D. C. Reynolds, C. W. Litton, and T. C. Collins, Phys. Status Solidi **9**, 645 (1965); **12**, 3 (1965); R. E. Halstead, in *The Physics and Chemistry of II-VI Compounds*, edited by M. Aven and J. S. Prener (John Wiley & Sons, Inc., New York, 1967).

[2] D. G. Thomas and J. J. Hopfield, Phys. Rev. **128**, 2135 (1962).

optical phonon replicas. Many such bands have been seen in CdS.[1,3–12] They are usually interpreted as "free-to-bound" transitions, which are thought of as the recombination of a free electron and a neutral acceptor, or as "bound-to-bound" transitions, which are thought of as donor-acceptor pair-recombination bands. In undoped vapor-grown CdS platelets, there are two commonly occurring bands. One of these, which peaks at 5125 Å, is thought to be a free-to-bound transition.[4,8,10] The other band, which peaks at 5176 Å, has been identified as a donor-acceptor pair-recombination band. [8,10,13] This identification is based upon the observation that, after pulse excitation, the band decays slowly and nonexponentially and shifts to lower energy in time in a manner that has been well established for the behavior of donor-acceptor pairs in GaP.[14] However, the studies of this band and the other numerous studies of the green-edge emission in CdS did not reveal the most striking feature of donor-acceptor pair-recombination bands which is the series of discrete pair lines due to the closely spaced donor-acceptor pairs. This is in contrast with GaP, the best understood of the wide bandgap semiconductors, where pair lines have been found to accompany essentially all of the numerous donor-acceptor pair bands that have been thus far observed.[15–18]

There are several reasons why pair lines should be more difficult to observe in CdS than in GaP. First, the pair series in hexagonal (wurtzite) CdS is expected to contain roughly four times as many lines as the cubic (zinc-blende) GaP, because the maximum number of symmetry-equivalent pairs is only six for wurtzite, while it is 24 for zinc blende. Second, the luminescence from excitons bound to donors and acceptors is much stronger in CdS than in GaP. Phonon replicas and other broad emission bands associated with the bound exciton emission tend to overlap and obscure the weaker pair lines. Third, the emission lines in CdS become concentration-broadened when impurities are added in growth. In general, the strain-free samples possessing sharp lines are samples which have not been intentionally doped. In these samples, the bound excitons are much stronger than the pair bands.

In this paper, we report the first observation of discrete donor-acceptor pair lines in CdS. This is also the first observation of discrete donor-acceptor pairs in hexagonal, II-VI semiconductors. Pair lines have been observed in numerous III-V compounds,[14–20] in cubic and hexagonal SiC,[21,22] and recently in ZnSe, a cubic II-VI semiconductor.[23] We have observed a number of different series of pair lines. Our two best examples appear to converge on the distant pair peaks at 5176 Å. In Sec. II, we discuss our experimental methods. The pair spectrum and its correlation with a distant pair peak and with bound excitons are discussed in Sec. III. Section IV and the Appendices deal with the Zeeman experiments, confirming that the lines are closely spaced donor-acceptor pairs. In Sec. V, we discuss a theoretical wurtzite pair spectrum and compare it with what is found experimentally and with a theoretical zinc-blende spectrum. Finally, in Sec. VI we summarize our results and list some of the remaining problems concerning donor-acceptor pairs in CdS.

II. EXPERIMENTAL METHODS

The observation of the donor-acceptor pair lines was greatly aided by the use of an argon-ion laser. The pairs were excited with 20–200 mW of focused 4880 Å argon-laser radiation directed along the c axis of the crystal. The pair lines were observed photographically using a 2-m Bausch and Lomb spectrograph with a dispersion of 1.7 Å/mm. The luminescence was observed through a polarizer crossed to the laser polarization to reduce the intensity of the reflected laser light. The 4880 Å laser line is higher in energy than the I_1 line and the close pairs, but lower in energy than the I_2 lines and other transitions of bound and free excitons. The 4880 Å light excited the I_1 line and the pair lines selectively, without exciting the other bound excitons. All the excitons and also the pair lines could be excited by using the above band gap 4765 Å argon-laser line. However, the pair lines were excited more strongly relative to a broad background luminescence using the 4880 Å line. Even with the 4880 Å excitation, this broad background luminescence made observation of the pair lines difficult and in many cases impossible.

The samples were strain-free platelets of CdS, grown from the vapor using an argon transport gas. Pair lines

---

[3] F. A. Kroger, Physica **7**, 1 (1940).

[4] L. S. Pedrotti and D. C. Reynolds, Phys. Rev. **120**, 1664 (1960).

[5] S. Ibaki and A. Ohso, J. Phys. Chem. Solids **27**, 1753 (1966).

[6] G. Condas and J. H. Yee, Appl. Phys. Letters **9**, 188 (1966).

[7] O. Goede and E. Gutsche, Phys. Status Solidi **17**, 911 (1966).

[8] K. Colbow, Phys. Rev. **141**, 742 (1966).

[9] S. Iida and M. Toyama, J. Phys. Soc. Japan **22**, 343 (1967).

[10] D. G. Thomas, R. Dingle, and J. D. Cuthbert, in *II-VI Semiconducting Compounds*, edited by D. G. Thomas (W. A. Benjamin, Inc., New York, 1967) p. 863.

[11] C. Z. van Doorn, J. Phys. Chem. Solids **29**, 599 (1968).

[12] D. L. Kingston, L. C. Greene, and W. Craft, J. Appl. Phys. **39**, 5949 (1968).

[13] D. G. Thomas, J. J. Hopfield, and K. Colbow, in *Proceedings of the Symposium on Radiative Recombination in Semiconductors* (Dunod Cie., Paris, 1964), p. 67.

[14] D. G. Thomas, J. J. Hopfield, and W. M. Augustyniak, Phys. Rev. **140**, A202 (1965).

[15] D. G. Thomas, M. Gershenzon, and F. A. Trumbore, Phys. Rev. **133**, A269 (1964).

[16] F. A. Trumbore and D. G. Thomas, Phys. Rev. **137**, A1030 (1965).

[17] P. J. Dean, C. H. Henry, and C. J. Frosch, Phys. Rev. **168**, 812 (1968).

[18] P. J. Dean, C. J. Frosch, and C. H. Henry, J. Appl. Phys. **39**, 5631 (1968).

[19] F. M. Ryan and R. C. Miller, Phys. Rev. **148**, 858 (1966).

[20] M. R. Lorentz, T. N. Morgan, G. D. Pettit, and W. J. Turner, Phys. Rev. **168**, 902 (1968).

[21] W. J. Choyke, D. R. Hamilton, and L. Patrick, Phys. Rev. **133**, A1163 (1964).

[22] W. J. Choyke, Materials Research Bulletin (to be published).

[23] P. J. Dean and J. L. Merz, Phys. Rev. (to be published).

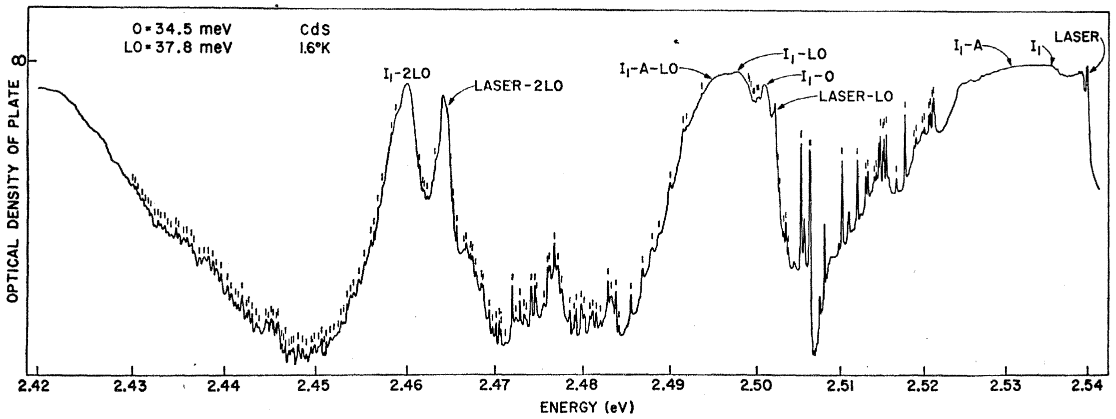

FIG. 1. Donor-acceptor pair-line spectrum measured at 1.6°K in an undoped CdS platelet. The sample was excited by 20 mW of focused laser 4880 Å. The lines thought to be pair lines are marked with vertical lines. A and O refer to acoustic and optical phonon replicas of the I_1 line.

have only been observed thus far in samples in which no impurities have been intentionally added.

III. EXPERIMENTAL RESULTS

Figure 1 shows our best example of a spectrum of donor-acceptor pair lines. The spectrum has nearly 170 resolvable lines. The lines converge into a broad band at lower energies. Large portions of the spectrum are obscured by the optical phonon replicas of the I_1 line labeled A, LO, and O and also by Raman scattering at LO and 2LO. We were only able to observe the pair lines in liquid helium pumped below the λ transition. At a helium temperature of 4.2°K, the lines were not observable and we believe that the focused laser radiation caused the sample to heat up considerably above 4.2°K.

Note in proof: Recently D. C. Reynolds and T. C. Collins have submitted a paper to the Phys. Rev. reporting a discrete donor-acceptor pair line spectrum in CdS. The spectrum is similar to, but not the same as the one aeported here.

Figure 2 shows the higher-energy pair lines excited with (a) focused 4880 Å laser light and (b) with focused 4765 Å laser light. This figure demonstrates that the pair lines are much more strongly excited, relative to the broad background, by the 4880 Å light than by the 4765 Å radiation.

Figure 3 shows the green-edge emission under focused and unfocused 4880 Å excitation. With 10 mW of unfocused laser light only, the distant pair band[8,10,13] at 5176 Å and the band at 5125 Å, which is thought to be a free-to-bound transition.[4,8,10] show up strongly. With focused laser radiation, the distant pair band shifts to higher energy and can no longer be resolved from the free-to-bound band. The I_1 line and its phonon replicas come in quite strongly and the discrete pair lines can be observed superimposed upon a broad background. The background is due, at least in part, to the phonon replicas of the I_1 line. The distant pair peak near 5176 Å occurs in all samples showing this pair spectrum.

Figure 4 shows the spectrum of bound excitons in the sample giving rise to the pair lines. This spectrum was excited with 40 mW of focused 4765 Å laser light. The lines labeled *a*–*g* are closely spaced in energy and have the appropriate energy to be excitons bound to neutral donors, i.e., I_2 lines. Lines *a*, *b*, *c*, and *f* behave in a magnetic field like the I_2 lines studied by Thomas and Hopfield, while *g* does not. A survey of 17 samples from different growths, all showing the same spectrum of pair lines, showed that the pair-line spectrum correlated with the I_1 line at 4888.52 Å and the I_2 line at 4869.30 Å (line *b* in Fig. 4). Another pair-line spectrum, not shown in the figures, of which we have examples from three different growths, appears to correlate with the same I_1 line and an I_2 line at 4869.17 Å. The distant pair peak in these samples was also near 5176 Å. Several other series of pair lines were observed in samples having the same I_1 line. We did not have enough examples of these series to correlate them with an I_2 line. Another common I_1 line occurs at 4888.19 Å. Thus far we have not been able to find any pair-line spectra which correlate with this I_1 line. (The wavelengths quoted here are in air at 15°C and were measured using an Fe-Ne calibration lamp.)

We believe that all the prominent lines in Fig. 1 are due to a single pair spectrum. This is so because the well-resolved high-energy pair lines were observed in many samples from different growths with the same intensity ratios. It is surprising that we did not observe many more pair-line spectra since the undoped vapor-grown platelets exhibit many different I_2 lines in their luminescence and two prominent I_1 lines.

IV. ZEEMAN SPLITTINGS OF PAIR LINES

Many of the prominent pair lines shown in Fig. 1, lying between I_1 and I_1—LO, are strong enough and sufficiently well isolated from neighboring pair lines to give an observable Zeeman pattern. A good example of such a Zeeman pattern is shown in Fig. 5 for $\mathbf{H}\|c$ and $\mathbf{H}\perp c$. A given donor-acceptor pair will have an

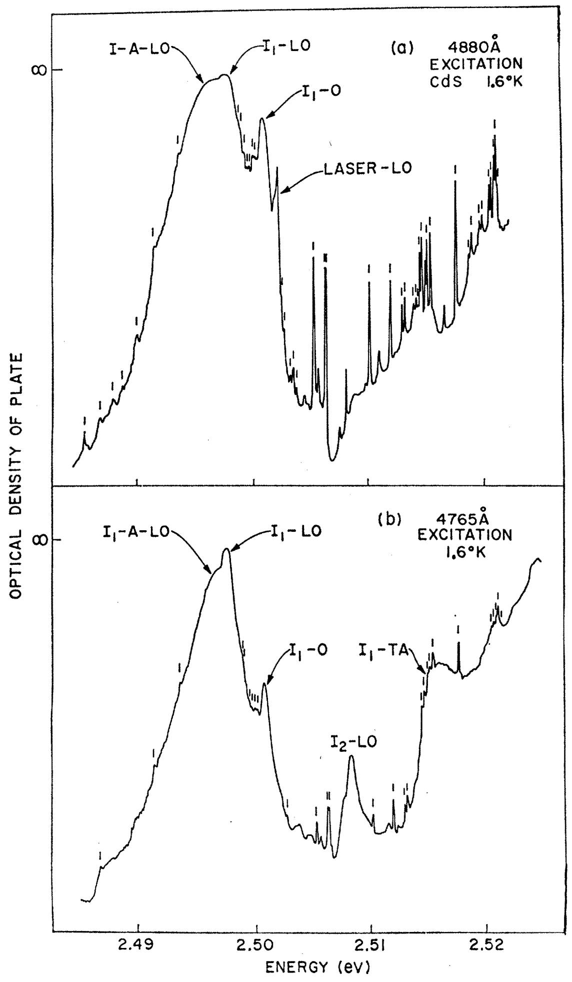

FIG. 2. Comparison of the donor-acceptor pair-line spectrum measured with 4880 and 4765 Å. The same pair lines are found in both cases, but the lines excited with 4880 Å stand out much stronger relative to the broad background.

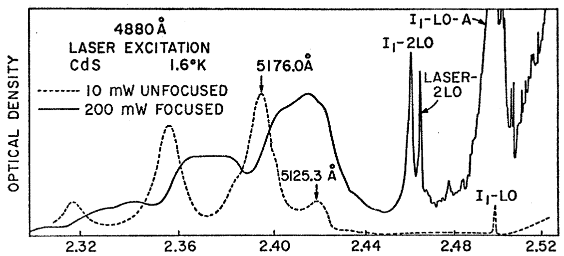

FIG. 3. Comparison of donor-acceptor pairs excited with focused and unfocused laser light. For unfocused excitation the distant pair peak at 5176 Å and the free-to-bound transition at 5125 Å stand out. For focused excitation, the distant pair peak shifts to higher energies and the spectra are dominated by the phonon replicas of the I_1 line.

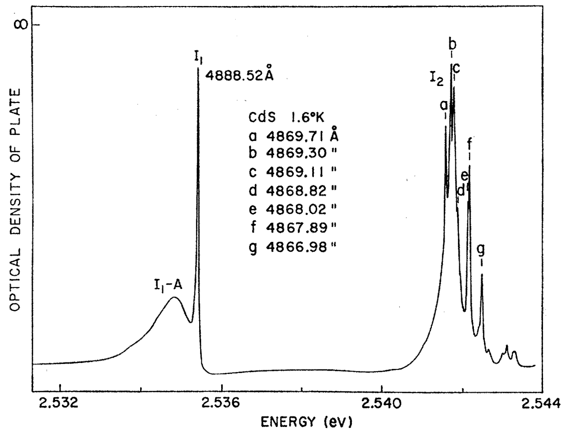

FIG. 4. The blue-edge emission in the same crystal giving the pair-line spectrum excited with 40 mW of focused laser light at 4765 Å. The I_1 line and line (b) of the I_2 lines correlate with the presence of the pair lines.

electronic degeneracy of 4 [(2 for the electron)×(2 for the hole)]. For the CdS wurtzite lattice, there can be as many as 12 pairs which are crystallographically equivalent, but which have different orientations with respect to the external magnetic field.[24] On the basis of symmetry, therefore, the magnetic splittings could be dreadfully complicated. This was not observed, however. Each of the crystallographically equivalent donor-acceptor pairs gave the same splitting in a magnetic field. That is, each pair ("pair" hereafter refers to the set of crystallographically equivalent pairs) splits into four lines, as shown in Figs. 5 and 6. The data in these figures were fitted quite adequately by the solid theoretical curves. The theory of the Zeeman splittings is presented in Appendix A. The splittings of the pair lines are due to the *j-j* coupling between the electron and hole and the Zeeman interactions of the

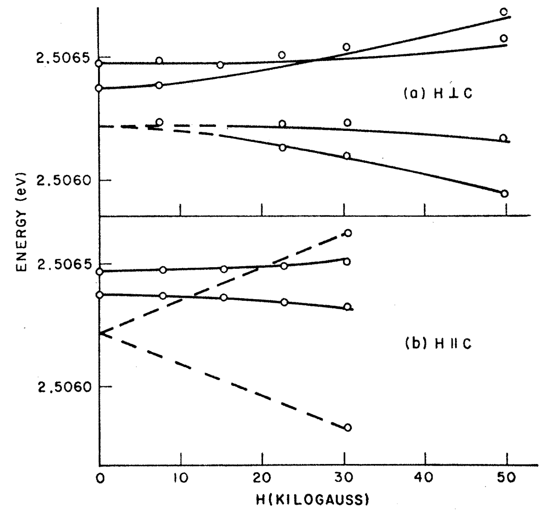

FIG. 5. Magnetic splittings of a typical pair line. The solid and dashed lines are calculated from Eqs. (4.1)–(4.4).

---

[24] The number 12 results because there are six symmetry operations in the C_{3v} point group of a substitutional donor (acceptor) which bring symmetry-equivalent pair sites into each other and because there are two inequivalent donor (acceptor) sites in the unit cell which are identical except for a rotation of the crystal by 60° about the *c* axis and a nonprimitive translation.

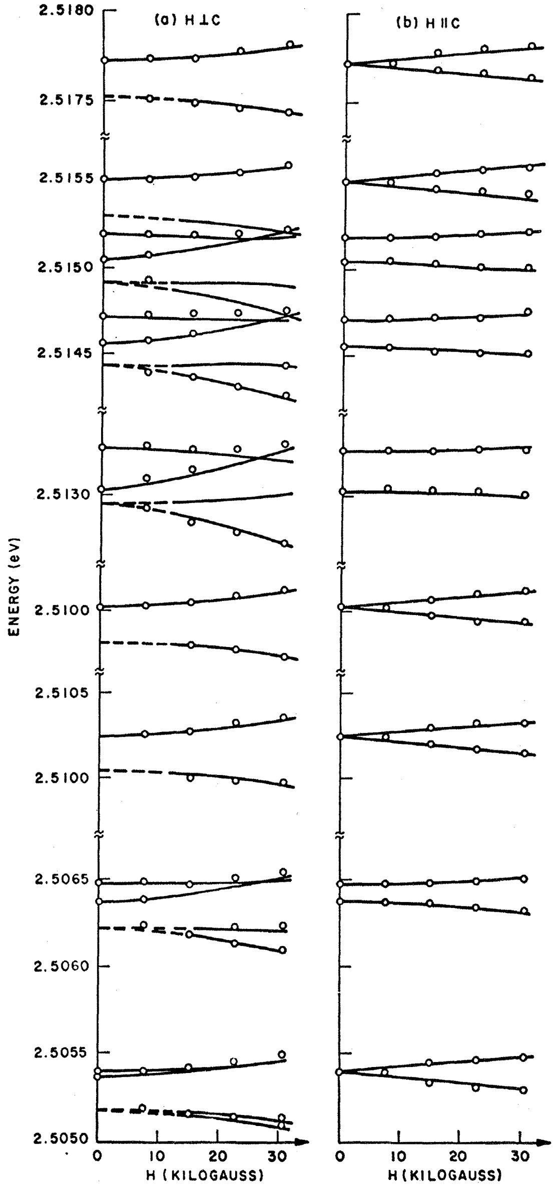

FIG. 6. Magnetic splittings of nine consecutive pair lines. The dashed and solid curves are calculated from Eqs. (4.1)–(4.4).

electron and the hole with the external magnetic field. In effect, because the donor is close to the acceptor, it acts as a perturbing crystal field which lowers the symmetry of the acceptor site and causes a mixing of the low-lying acceptor excited states into the ground state. This mixing was sufficiently weak that the g value of the acceptor for $\mathbf{H}\|(c$ axis) was unchanged from its value for an isolated acceptor. We were able to predict the magnetic behavior of the pair lines using two parameters: A, the j-j coupling constant and $|D|$, a crystal-field splitting. Constants A and $|D|$ were evaluated from the zero-field splittings. In zero field, the electron and hole j-j coupling splits the four states into an allowed doublet and a forbidden doublet separated by A. As a result of the mixing of the hole states by the crystal field the matrix elements of angular momentum of the hole ⊥ to the c axis are no longer zero, as they are for an isolated acceptor. This results in an additional j-j coupling term, which splits the allowed doublet by $|D|$ in zero field. For H parallel to the c axis, the states split as

$$E=\tfrac{1}{2}\{A\pm[(g_{h\|}-g_e)^2(\beta H)^2+|D|^2]^{1/2}\}\,,\quad \text{allowed} \qquad (4.1)$$

$$E=\tfrac{1}{2}[-A\pm(g_{h\|}+g_e)\beta H]\,,\quad \text{forbidden} \qquad (4.2)$$

where $g_e=1.76$ and $g_{h\|}=2.76$ are the g values of an isolated donor and acceptor. For H perpendicular to the c axis, the behavior is more complicated. As the field is turned on, both transitions become allowed. The calculated splittings are given by

$$E=\frac{1}{2}\left\{[A^2+(g_e\beta H)^2]^{1/2}\pm|D|\left[1+\frac{[A-(2\alpha/A)(g_e\beta H)^2]}{[A^2+(g_e\beta H)^2]^{1/2}}\right]\right\}, \qquad (4.3)$$

$$E=-\frac{1}{2}\left\{[A^2+(g_e\beta H)^2]^{1/2}\pm|D|\left[1-\frac{[A-(2\alpha/A)(g_e\beta H)^2]}{[A^2+(g_e\beta H)^2]^{1/2}}\right]\right\}. \qquad (4.4)$$

The constant $\alpha=0.78$ is calculated in Appendix A. In zero field the allowed transition is split by $|D|$, while the forbidden transition has no splitting. As $H_\perp$ is increased the allowed lines move together and cross at about 28 kG, while the forbidden lines move apart. This feature, which is shown most clearly in Fig. 5(a), was observed for all the pair lines studied. A common value of $A=0.20$ meV was used for the splitting by j-j coupling. The value of the crystal-field splitting $|D|$ was different for each pair studied and was found from the zero-field splitting of the allowed doublet. It varied from 0 to 0.25 meV. We are unable to predict how the splitting $|D|$ varies from one pair to the next. In Fig. 6 we show the Zeeman splittings of nine consecutive pair lines. Only three lines in Fig. 6(a) are not verified with data points. In all cases they are lines of relatively weak pairs, which are forbidden for $H_\perp=0$. The higher-energy line of the forbidden doublets become weak, apparently due to thermalization, as $H_\perp$ was turned up and the doublet split apart. This effect we believe accounts for why we could not observe the lines near 2.5130 and 2.5149 eV.

Thomas and Hopfield[2] studied the I_3 transition, which is an exciton bound to an ionized donor. This transition is analogous to the high-energy pair transitions. Both centers consist of an electron and hole bound to an ionized site. The magnetic behavior of the I_3 line is the same as it is for the pair lines, except for I_3 there is no crystal-field splitting and the hole g value is $g_{h\|}=1.76$ instead of the acceptor g value of $g_{h\|}=2.76$. The j-j coupling for the I_3 line has the same sign as for

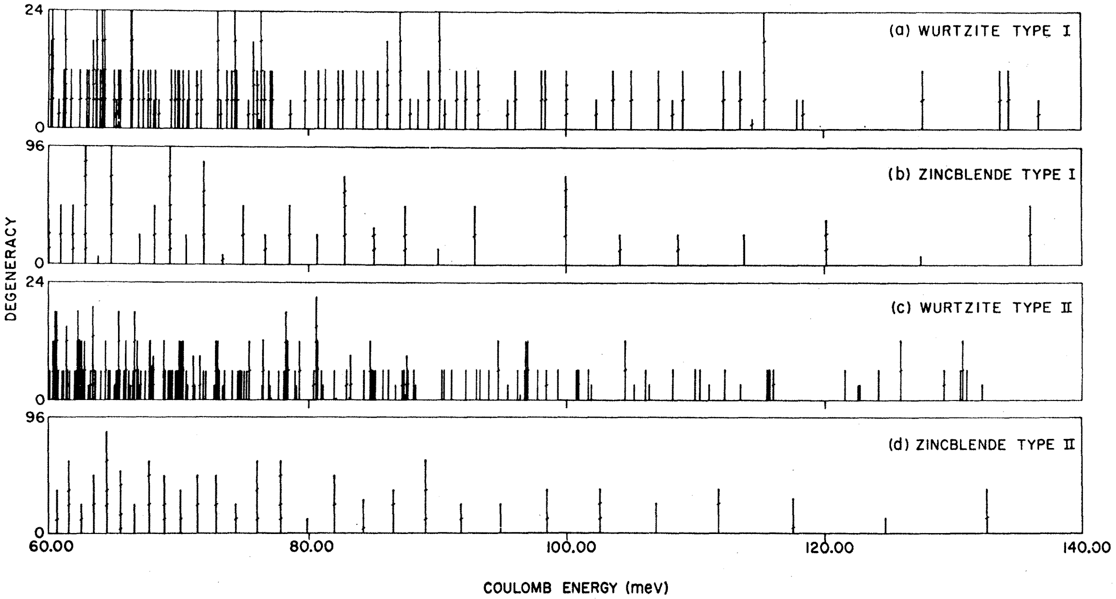

FIG. 7. Comparison of the theoretical pair spectra for wurtzite and zinc blende: (a) Type-I, wurtzite, (b) Type-I, zinc blende, (c) Type-II, wurtzite, (d) Type-II, zinc blende. We use $\epsilon_\perp=9.35$, $\epsilon_{\parallel}=10.35$, (Ref. 28) $c=6.713$ Å, $a=4.136$ Å for wurtzite and $\epsilon=9.68$, $a=5.837$ Å for zinc blende. The breaks in the vertical lines distinguish between inequivalent pair lines with the same Coulomb energy.

the pair lines and gives a splitting of $A=0.31$ meV between the allowed and forbidden doublets. Thomas and Hopfield argue that this splitting is proportional to the probability of finding the electron and hole on the same atom. For the high-energy pair lines, the donor-acceptor separation of roughly 10 Å is small compared to the donor Bohr radius of 25 Å.[25] Since, for these pair lines, the electron and hole envelope functions are greatly overlapping, it is not surprising that the j-j coupling for the pair is only slightly less than for a weakly bound exciton. In Appendix B, we roughly estimate

$$A\,(\text{pair})/A\,(\text{exciton})\approx 0.45\,.$$

The observed ratio is 0.64.

V. CALCULATION OF COULOMB SHIFT OF PAIR LINES

In this section we present a calculation of the pair-line spectrum for wurtzite CdS, taking into account Coulomb interactions only. We will compare this spectrum to a zinc-blende pair spectrum and with experiment. A wurtzite pair spectrum is more complicated than a zinc-blende pair spectrum because of two factors. The first is simply geometrical, in that the number of symmetry-equivalent pairs is greatly reduced in wurtzite, where a substitutional impurity has C_{3v} symmetry as opposed to T_d symmetry for a substitutional impurity in a zinc-blende lattice. The maximum number of symmetry-equivalent pairs in C_{3v} is only six, as contrasted with 24 for T_d. The second factor is the anisotropy of the dielectric constant. The Coulomb energy of a pair of point charges in a uniaxial crystal like CdS is given by[26]

$$E=e^2/[\epsilon_\perp\epsilon_{\parallel}(x^2+y^2)+\epsilon_\perp{}^2z^2]^{1/2}\,, \tag{5.1}$$

where $\epsilon_\perp$ is the dielectric constant perpendicular to the c axis and $\epsilon_{\parallel}$ is the dielectric constant parallel to the c axis (here taken along the z direction).

It is impossible to catalog the D-A separations in wurtzite simply according to shell numbers as in zinc blende because the separations depend on the c/a ratio. For any particular c/a ratio, however, it is straightforward to generate all desired separation vectors.

The primitive lattice vectors for wurtzite are[27]:

$$\mathbf{t}_1=\tfrac{1}{2}a(\sqrt{3}\mathbf{i}-\mathbf{j}),\quad \mathbf{t}_2=a\mathbf{j},\quad \mathbf{t}_3=c\mathbf{k}, \tag{5.2}$$

where $\mathbf{i}$, $\mathbf{j}$, $\mathbf{k}$ are unit vectors along the x, y, z directions, respectively. Any lattice vector is a simple linear combination of these primitive vectors with integer coefficients.

$$\mathbf{R}=n_1\mathbf{t}_1+n_2\mathbf{t}_2+n_3\mathbf{t}_3\,, \tag{5.3}$$

or, more symbolically,

$$\mathbf{R}=(n_1,n_2,n_3)\,. \tag{5.4}$$

Within the primitive cell, using CdS for example, two cadmium atoms are located at $(\frac{1}{3},\frac{2}{3},0)$ and $(\frac{2}{3},\frac{1}{3},\frac{1}{2})$ and two sulfur atoms are located at $(\frac{1}{3},\frac{2}{3},u)$ and $(\frac{2}{3},\frac{1}{3},u)$. The constant u is very close to $\frac{3}{8}$ for all wurtzite crystals.

---

[25] D. Schecter, Phys. Letters **26A**, 622 (1968).

[26] J. J. Hopfield and D. G. Thomas, Phys. Rev. **122**, 35 (1961).

[27] J. C. Slater, *Quantum Theory of Molecules and Solids* (McGraw-Hill Book Co., New York, 1965) Vol. 2, p. 60.

TABLE I. Comparison of calculated and observed pair-line densities.

E_{Coulomb} (meV)	Experiment (lines/meV)	Wurtzite type-I (lines/meV)	Wurtzite type-II (lines/meV)
128	0.6	0.5	0.7
88	1.6	2.9	2.7

For a type-I pair spectrum, in which both the donor and the acceptor occupy the same type lattice site (the Cd site or the S site), the separation vectors are given by the two expressions

$$\mathbf{R}_1=(n_1,n_2,n_3)\,,$$
$$\mathbf{R}_2=(n_1+\tfrac{1}{3},n_2-\tfrac{1}{3},n_2+\tfrac{1}{2})\,, \qquad (5.5)$$

where n_1, n_2, and n_3 run over all integer values.

For a type-II spectrum in which the donor occupies the opposite type site from that occupied by the acceptor, the separation vectors are given by

$$\mathbf{R}_1=(n_1,n_2,n_3+u)\,,$$
$$\mathbf{R}_2=(n_1=\tfrac{1}{3},n_2-\tfrac{1}{3},n_3+u+\tfrac{1}{2})\,. \qquad (5.6)$$

Figure 7 shows theoretical type-I and type-II pair spectra for CdS along with the corresponding spectra in a hypothetical zinc-blende CdS crystal for comparison. The breaks in a vertical line indicate that the line is a superposition of several symmetry-inequivalent pair lines with the same Coulomb energy. In the real crystal, these symmetry-inequivalent pair lines will split apart.

We were not able to identify the pair lines observed experimentally. Such an identification, which has been done many times for pair-like spectra in zinc-blende crystals, is much more difficult for pair lines in wurtzite CdS, for several reasons. First, Fig. 7 clearly shows that the pair-line spectrum due to Coulomb interactions is much more complicated for wurtzite than for zinc-blende. The calculated wurtzite spectrum is sensitive to the ratio of $\epsilon_\perp/\epsilon_\parallel$, which may not be accurately known for CdS. The symmetry-inequivalent pair lines split and shift about because of short-range non-Coulomb interactions. In the numerous studies of pair lines in GaP and other zinc-blende crystals, these interactions have been sufficiently small that the pair lines have been left in the same order as is predicted by calculations of the Coulomb energy. In other words, the pair lines of different radial shells do not overlap. This may not be the case in CdS, where the Coulomb spectrum is much more complicated and the resolvable pair lines correspond to strongly overlapping donor-acceptor pairs. Finally, identification was difficult because the phonon replicas from the I_1 line obscured much of the experimental spectrum.

Not being able to identify the pair lines, we have settled for a cruder comparison of theory and experiment. We have measured the density of pair lines in Fig. 1 in a 20-meV interval near 2.513 eV and in a 10-meV interval near 2.473 meV. These are the two regions of the spectrum where the donor-acceptor pair lines stand out most clearly. We wish to compare these densities with the calculated pair-line densities at the same Coulomb energy. If we take the distant pair peak to be at $E=2.395$ eV (5176 Å) and estimate the Coulomb energy for the pairs contributing to this peak to be about 10 meV, then the Coulomb energies associated with the pair lines will be 128 and 88 meV where we measured the pair-line densities. Table I compares the measured and calculated pair-line densities at these energies. The measured number of pair lines at 88 meV is smaller than expected, indicating that we were not able to resolve all of the pair lines in this region. The comparison between theory and experiment is rough because of the uncertainties in the values of $\epsilon_\perp$ and $\epsilon_\parallel$.[28] The magnitude of the pair-line densities agrees roughly with what is predicted. It should be emphasized, that the observed line densities were not greater than the theoretical line densities. This confirms that we are dealing with a single pair-line spectrum. It also shows that both the donor and acceptor sites have C_{3v} symmetry. If the symmetry of the sites were lower, for example, if the acceptor were a complex not oriented along the c axis, the calculated spectrum would have had about three times as many lines and would not have agreed with experiment.

VI. SUMMARY AND DISCUSSION

We report the first observation of discrete donor-acceptor pair lines in CdS. This is the first time that discrete pair lines have been studied in a II-VI compound of wurtzite structure. We were able to correlate the pair spectrum with the distant pair peak at 5176 Å and with a single I_1 line and a single I_2 line. A second pair spectrum, which was observed in fewer different growths, correlated with the same distant pair peak, with the same I_1 line and with a different I_2 line. We were not able to identify the pair lines. We were able to show, however, that the density of pair lines was roughly in agreement with what was predicted theoretically for a single pair spectrum. The Zeeman experiments confirmed that we were dealing with donor-acceptor pairs. It showed that many of the high-energy pair lines were doublets in zero field. The Zeeman measurements allowed us to measure the j-j coupling for the higher-energy pair lines. We showed that the magnitude of this coupling was reasonable for pairs in

---

[28] In the calculated spectrum we have used the room-temperature dielectric constants for CdS $\epsilon_\parallel=10.33$ and $\epsilon_\perp=9.35$ measured by D. Berlincourt, H. Jaffe, and L. R. Shiozawa, Phys. Rev. **129**, 1009 (1963). The agreement is worse if one uses the values of $\epsilon_\parallel$ and $\epsilon_\perp$ measured at liquid-nitrogen temperature, which are about 9% smaller. However, it has been the experience in both GaP and ZnSe that for close pairs the measured Coulomb energy is smaller than that given by $e^2/\epsilon_0 R$. Hence, the effective dielectric constant for close pairs is greater than the static dielectric constant ϵ_0, and it is reasonable that room-temperature dielectric constants fit the data better than the low-temperature values.

which the donor strongly overlaps the acceptor, which is what is expected for the high-energy pair lines. We are able to fit the observed magnetic splittings with a relatively simple theory.

A number of problems remain concerning the pair lines and the green-edge emission in CdS. First and foremost, the chemical nature of most of the donors and acceptors in CdS remains unknown. There appear to be very many I_2 lines in these undoped CdS crystals. It is not clear why we did not observe more than a few pair spectra. The band at 5126 Å is thought to be free to bound, yet we were able to observe this band at 1.6°K under conditions of weak excitation. It is difficult to understand why a free-to-bound transition should be present at 1.6°K and why this transition is as broad as a pair band.

ACKNOWLEDGMENTS

We would like to thank A. M. Sergent for his expert technical assistance and J. Shiever for growing a number of the crystals used in these experiments.

APPENDIX A: THEORY OF THE ZEEMAN SPLITTINGS OF THE PAIR LINES

Let us begin by considering a distant donor-acceptor pair in a cubic zinc-blende semiconductor, such as cubic CdS or GaP. The valence band is split by spin-orbit coupling into an upper fourfold degenerate valence band ($J=\frac{3}{2}$) and a lower twofold degenerate valence band with $J=\frac{1}{2}$. We may write an effective Hamiltonian which describes the coupling of the electron and the hole:

$$\mathcal{H}=\tfrac{1}{2}g_e\beta\mathbf{H}\cdot\boldsymbol{\sigma}+g_h\beta\mathbf{H}\cdot\mathbf{J}+a_J\mathbf{J}\cdot\boldsymbol{\sigma}, \qquad \text{(A1)}$$

where $\mathbf{J}$ is the angular momentum of the $J=\frac{3}{2}$ hole and the spin of the electron is $\frac{1}{2}\boldsymbol{\sigma}$.[29] The terms included in (A1) are the Zeeman interaction of the electron, the Zeeman interaction of the hole, and the *j-j* coupling of the electron and hole, discussed by Thomas and Hopfield.[2] Hopfield has discussed the zone-center valence-band wave functions for wurtzite in the quasicubic approximation. In this approximation, the wurtzite crystal is thought of as a strained zinc-blende crystal. To represent CdS, the strain splitting of the valence band must be 15 meV. We may expect that the strain will split the acceptor ground state by a similar amount. The strain splitting will also mix excited states of the acceptor into the Γ_8 ground-state manifold. Such admixtures will alter the constants and the form of the Hamiltonian. These changes should be small, because the strain splitting is small compared to the binding energy of the acceptor (~170 meV). Changes in the constants are unimportant since g_e and g_h are determined experimentally from magnetic studies of the I_1 and I_2 lines and a_J will be determined from our experimental data.

Consider the effect of bringing the donor ion close to the acceptor. First of all, this will increase the *j-j* coupling constant a_J, which depends upon the overlap of the electron and hole wave function. We estimate the magnitude of this constant in Appendix B. The electrostatic Coulomb interaction between the donor and the acceptor shifts the energies of the donor and acceptor ground states and thereby gives rise to the pair lines. This interaction cannot split these ground states which are Kramer's doublets. The major effect of this interaction will be to lower the symmetry of the acceptor site and to mix the low-lying excited state of the acceptor with the ground state; such an admixture will not alter the Hamiltonian. If we denote the ground state of the isolated acceptor as $|\pm\frac{3}{2}\rangle$ and the acceptor states split off from the ground state by strain as $|\pm\frac{1}{2}\rangle$, we can write the perturbed acceptor ground state $|\varphi_{\pm 3/2}\rangle$:

$$\begin{aligned}|\varphi_{3/2}\rangle&=|\tfrac{3}{2}\rangle-\Delta^{-1}[|\tfrac{1}{2}\rangle\langle\tfrac{1}{2}|V|\tfrac{3}{2}\rangle+|-\tfrac{1}{2}\rangle\langle-\tfrac{1}{2}|V|\tfrac{3}{2}\rangle],\\ |\varphi_{-3/2}\rangle&=|-\tfrac{3}{2}\rangle-\Delta^{-1}[|-\tfrac{1}{2}\rangle\langle-\tfrac{1}{2}|V|-\tfrac{3}{2}\rangle\\ &\qquad+|\tfrac{1}{2}\rangle\langle\tfrac{1}{2}|V|-\tfrac{3}{2}\rangle], \qquad \text{(A2)}\end{aligned}$$

where Δ is the strain splitting of the isolated acceptor ground state and V is an effective crystal field due to the presence of the neighboring donor. The states $|\pm\frac{3}{2}\rangle$ and $|\pm\frac{1}{2}\rangle$ are eigenstates of J_z. Potential V can also alter the Hamiltonian by mixing the ground state of the acceptor with higher excited states. For example, the g splitting of the acceptor ground state for $H\|c$ axis (taken in the z direction) could change. We find experimentally that $g_{h\|}$ and g_e are the same for the pair lines as for isolated donors and acceptors. The stability of the hole g value is quite surprising, but it indicates that the mixing of excited states of the acceptor into the ground state is small and that $\mathcal{H}$ [Eq. (A1)] still applies. We may write $\mathcal{H}$ more explicitly:

$$\begin{aligned}\mathcal{H}=&\tfrac{1}{2}g_e\beta H_z\sigma_z+\tfrac{1}{2}g_e\beta(\tfrac{1}{2}H_+\sigma_-+\tfrac{1}{2}H_-\sigma_+)+g_h\beta H_zJ_z+\tfrac{1}{2}g_H\beta\\ &\times(H_+J_-+H_-J_+)+a_J(J_z\sigma_z+\tfrac{1}{2}J_+\sigma_-+\tfrac{1}{2}J_-\sigma_+), \qquad \text{(A3)}\end{aligned}$$

where $H_\pm=H_x\pm iH_y$, etc. The splittings of the pair lines are given by the eigenvalues of $\mathcal{H}$. The problem reduces to evaluating the matrix elements of J_z and $J_\pm$ within the states $|\varphi\pm\frac{3}{2}\rangle$. Some of these matrix elements are related, while others are considered to be parameters and have to be determined by experiment. The parameters are

$$\begin{aligned}A&=-a_J\langle\varphi_{3/2}|J_z|\varphi_{3/2}\rangle,\\ C&=a_J\langle\varphi_{3/2}|J_-|\varphi_{3/2}\rangle, \qquad \text{(A4)}\\ D&=a_J\langle\varphi_{-3/2}|J_-|\varphi_{3/2}\rangle.\end{aligned}$$

We take g_e to be 1.76, the known g value of the electron. For an isolated acceptor matrix elements C and D would be zero. The effect of the perturbing donor is to produce

---

[29] This is not the most general Hamiltonian, which can include terms linear in H but nonlinear in $\mathbf{J}$ and $\boldsymbol{\sigma}$. For example, see Y. Yafet and D. G. Thomas, Phys. Rev. 131, 2405 (1963). Such terms are small and can be usually neglected, except in refined experiments.

nonzero matrix elements of $J_{\pm}$. To first order in V/Δ, $\langle\varphi_{3/2}|J_z|\varphi_{3/2}\rangle\approx\langle\frac{3}{2}|J_z|\frac{3}{2}\rangle$. This matrix element is related to the g value of an isolated acceptor, $g_{h\parallel}=2.76$, by

$$g_{h\parallel}=2.76=2g_h\langle\tfrac{3}{2}|J_z|\tfrac{3}{2}\rangle=-2g_hA/a_J. \qquad \text{(A5)}$$

For $H\perp c$ axis, the matrix elements of the hole Zeeman interaction can be written in terms of the electron Zeeman interaction

$$\begin{aligned}\tfrac{1}{2}g_h\beta H_+\langle\varphi_{-3/2}|J_-|\varphi_{3/2}\rangle&=\tfrac{1}{2}g_h\beta H_+D/a_J\\&=-\alpha(\tfrac{1}{2}g_e\beta H_+)D/A\,, \qquad \text{(A6)}\end{aligned}$$

where

$$\alpha=g_{h\parallel}/2g_e=2.76/2(1.76)=0.78. \qquad \text{(A7)}$$

Similarly, the diagonal matrix element

$$\begin{aligned}\tfrac{1}{2}g_h\beta\langle\varphi_{3/2}|J_+H_-+J_-H_+|\varphi_{3/2}\rangle&=-\alpha(\tfrac{1}{2}g_e\beta H_+)C/A\\&+\text{c.c.}=-\alpha(g_e\beta/A)Re(CH_+)\,. \qquad \text{(A8)}\end{aligned}$$

If we write $H_+=He^{i\varphi_H}$ and $C=|C|e^{i\varphi_V}$, matrix element (A8) will be proportional to $\cos(\varphi_H+\varphi_V)$. Simple models of the electrostatic interaction show that φ_V depends upon the orientation of the pairs, whereas $|D|$ and $|C|$ do not. Because of this matrix element, there may be as many as 12 crystallographically equivalent pairs, all having different orientations, which will have different Zeeman splittings. This is not what is observed. Experimentally, each pair line splits into four lines when a magnetic field is applied, i.e., pairs of different orientations have the same Zeeman splittings. From this we can only conclude that $|C|$ must be negligible compared to $|D|$ and we will drop this term in the remainder of our calculations. The matrix of $\mathcal{H}$ in the basis $|\varphi_{3/2},\frac{1}{2}\rangle$, etc., where the second quantum number refers to the electron wave function which is an eigenstate of σ_z, is given by

$$\begin{array}{cccccc} & |\varphi_{3/2},\frac{1}{2}\rangle & |\varphi_{3/2},-\frac{1}{2}\rangle & |\varphi_{-3/2},\frac{1}{2}\rangle & |\varphi_{-3/2},-\frac{1}{2}\rangle & \\ \frac{1}{2} & \left(\begin{array}{c} (g_{h\parallel}+g_e)\beta H_z-A \\ G_e \\ -\alpha DG_e/A \\ 0 \end{array}\right. & \begin{array}{c} G_e{}^* \\ (g_{h\parallel}-g_e)\beta H_z+A \\ D \\ -\alpha DG_e/A \end{array} & \begin{array}{c} -(\alpha D^*/A)G_e{}^* \\ D^* \\ (-g_{h\parallel}+g_e)\beta H_z+A \\ G_e \end{array} & \left.\begin{array}{c} 0 \\ -\alpha D^*G_e{}^*/A \\ G_e{}^* \\ (-g_{h\parallel}-g_e)\beta H_z-A \end{array}\right) & \begin{array}{l} |\varphi_{3/2},\frac{1}{2}\rangle \\ |\varphi_{3/2},-\frac{1}{2}\rangle \\ |\varphi_{-3/2},+\frac{1}{2}\rangle \\ |\varphi_{-3/2},-\frac{1}{2}\rangle \end{array} \end{array}$$

where $G_e=g_e\beta H_+$. For $\mathbf{H}\|(c$ axis) or $\mathbf{H}\perp(c$ axis), the quartic eigenvalue equation can be solved analytically. The solutions are presented in Sec. IV, where they are shown to agree well with the data.

APPENDIX B: ESTIMATE OF THE *j-j* COUPLING FOR A DONOR-ACCEPTOR PAIR

According to Thomas and Hopfield,[2] the *j-j* coupling is proportional to the probability of finding the electron and hole on the same atom. If the envelope function for the electron and hole is $\psi(\mathbf{r}_e,\mathbf{r}_h)$, then

$$A=\gamma\int|\psi(\mathbf{r},\mathbf{r})|^2dr\,, \qquad \text{(B1)}$$

where γ is a constant of proportionality. Equation (B1) should apply both to a weakly bound exciton such as that giving rise to I_3 and to the donor-acceptor pair lines, if we make the approximation that in both cases the hole wave function is derived from the uppermost valence band. For a weakly bound exciton,[30]

$$\psi(\mathbf{r}_e,\mathbf{r}_h)=f(\mathbf{R})\varphi(\mathbf{r}_e-\mathbf{r}_h)\,, \qquad \text{(B2)}$$

where $\mathbf{R}$ is the c.m. coordinate of the exciton and $\varphi(\mathbf{r}_e-\mathbf{r}_n)$ is the wave function describing the internal motion of the free exciton. In this case

$$A(\text{exciton})=\gamma|\varphi(0)|^2\int|f(\mathbf{R})|^2d\mathbf{R}=\gamma|\varphi(0)|^2. \qquad \text{(B3)}$$

For the case of a pair, we can write the pair

$$\psi(\mathbf{r}_e,\mathbf{r}_h)=f_e(\mathbf{r}_e)g_n(\mathbf{r}_h)\,. \qquad \text{(B4)}$$

In this case

$$A(\text{pair})=\gamma\int|f_e(\mathbf{r})|^2|g_h(\mathbf{r})|^2d\mathbf{r}. \qquad \text{(B5)}$$

If we assume that the hole envelope function is highly localized compared to that of the electron,

$$\begin{aligned}A(\text{pair})&\approx\gamma|f_e(0)|^2e^{-2R/a}\int|g_h(\mathbf{r})|^2dr\\&=\gamma|f_e(0)|^2e^{-2R/a}\,, \qquad \text{(B6)}\end{aligned}$$

where R is the separation between the donor and acceptor and a is the Bohr radius of the donor. $|f_e(0)|^2\approx|\varphi_e(0)|^2$, since both the donor and the exciton have about the same binding energy. The Bohr radius of the donor is about 25 Å. For the high-energy pairs we are considering, $R\approx10$ Å, so that from (B3) and (B6) we find

$$A(\text{pair})/A(\text{exciton})\approx e^{-2R/a}=0.45. \qquad \text{(B7)}$$

This crude estimate roughly agrees with the experimentally observed ratio of $A(\text{pair})/A(I_3)=0.20$ meV/0.31 meV$=0.64$, where $A(I_3)$ was measured from the data of Thomas and Hopfield.[2]

---

[30] E. I. Rashba and G. E. Gurgenishvili, Fiz. Tverd. Tela 4, 1029 (1962) [English transl.: Soviet Phys.—Solid State 4, 759 (1962)].